

## RESULTS OF A SEARCH FOR DAILY AND ANNUAL VARIATIONS OF $^{214}\text{Po}$ HALF-LIFE AT THE TWO-YEAR OBSERVATION PERIOD

*E. N. Alexeyev*<sup>1</sup>, *Yu. M. Gavrilyuk*<sup>1</sup>, *A. M. Gangapshev*<sup>1</sup>,  
*V. V. Kazalov*<sup>1</sup>, *V. V. Kuzminov*<sup>1,\*</sup>, *S. I. Panasenko*<sup>2</sup>,  
*S. S. Ratkevich*<sup>2</sup>

<sup>1</sup> Baksan Neutrino Observatory, Institute for Nuclear Research  
of the Russian Academy of Sciences, Russia

<sup>2</sup> V. N. Karazin Kharkiv National University, Kharkiv, Ukraine

The brief description of TAU-2 installation intended for a long-term monitoring of the half-life value  $\tau$  ( $\tau_{1/2}$ ) of  $^{214}\text{Po}$  is presented. The methods of measurement and processing of collected data are reported. The results of analysis of time series values  $\tau$  with different time step are presented. Total of measurement time was equal to 590 days. Averaged value of  $^{214}\text{Po}$  half-life was obtained  $\tau = (163.46 \pm 0.04) \mu\text{s}$ . The annual variation with an amplitude  $A = (8.9 \pm 2.3) \cdot 10^{-4}$ , solar-daily variation with an amplitude  $A_{\text{So}} = (7.5 \pm 1.2) \cdot 10^{-4}$ , lunar-daily variation with an amplitude  $A_L = (6.9 \pm 2.0) \cdot 10^{-4}$ , and sidereal-daily variation with an amplitude  $A_S = (7.2 \pm 1.2) \cdot 10^{-4}$  were found in a series of  $\tau$  values. The maximal values of amplitude are observed at the moments when the projections of the installation Earth location velocity vectors toward the source of possible variation achieve their maximal magnitudes.

PACS: 27.80.+w; 23.60.+e

### INTRODUCTION

Recently, in works intended to search for limits of the realization of the decay constant conservation law, a level of sensitivity not less than  $2 \cdot 10^{-4}$  was achieved for several radioactive isotopes. In [1] the authors showed that an amplitude of a possible annual variation of  $^{198}\text{Au}$  half-life ( $T_{1/2} = 2.69445$  days), that was measured with the relative uncertainty of  $\pm 7 \cdot 10^{-5}$ , does not exceed  $\pm 2 \cdot 10^{-4}$  of the central value. Variations with periods from several hours up to one year were excluded at the level of  $9.6 \cdot 10^{-5}$  (95% C.L.) during the measurements of  $^{137}\text{Cs}$  half-life ( $T_{1/2} = 10942$  days) in [2]. The annual variation was excluded

---

\*E-mail: bno\_vvk@mail.ru

at the level of  $8.5 \cdot 10^{-5}$  (95% C.L.). Variations of an activity with periods of 3–150 days were excluded at the level of  $2.6 \cdot 10^{-5}$  (99.7% C.L.) during the measurement of  $^{40}\text{K}$  activity in [3]. It was shown that an amplitude of the annual variation does not exceed  $6.1 \cdot 10^{-5}$  (95% C.L.). Variations of an activity with periods less than one year were excluded at the level of  $4 \cdot 10^{-5}$  during the measurement of  $^{232}\text{Th}$  activity in [3].

A count rate of the detector recording the source radiation was a subject of investigations in all mentioned works. A high sensitivity of the measurements was achieved by using a relatively high count rate ( $\sim 10^3 \text{ s}^{-1}$ ), of a control and stabilization of conditions of the measurements and by using additional arrangements for shield of the setups from outer background.

At the same time, the evidences for presence of the annual variations of different effects caused by a radiation of the investigated isotope are cited in a series of articles. For example, characteristics of the annual variations of the count rates of the detectors used for many years in measurements of  $^{32}\text{Si}$  and  $^{226}\text{Ra}$  sources activities are discussed in [4]. The amplitudes of variations are equal to  $\sim 1 \cdot 10^{-3}$ . The authors have examined possibilities of an appearing of such variations as a result of seasonal variations of the detector's characteristics or one of annual modulations of the isotope's decay rates themselves under the action of an unknown factor depending on the Earth–Sun distance. Results of continuous measurements of the decay rates of  $^{108}\text{Ag}$ ,  $^{133}\text{Ba}$ ,  $^{137}\text{Cs}$ ,  $^{152}\text{Eu}$ ,  $^{154}\text{Eu}$ ,  $^{85}\text{Kr}$ ,  $^{226}\text{Ra}$ , and  $^{90}\text{Sr}$  sources made in the Physikalisch-Technische Bundesanstalt (PTB) were discussed in [5,6]. Statistically significant annual variations with the amplitudes of  $(6.8\text{--}8.8) \cdot 10^{-4}$  were observed in the data for all these isotopes. The authors made a comparison between spectral power functions obtained from the data and the observed radial oscillations of the Sun's surface. However, the researchers from the PTB point in [7] at the laboratory factors capable to cause similar variations and warn against hasty conclusions about possible new physical phenomena.

It is clear that any conclusions about a possible new physical effect could be made after the complete exclusion of variations caused by influence of the known terrestrial geophysical, climatic, and meteorological factors on the source–detector couple count rate. Not all such factors could be detected and taken into account during the measurement and data processing. For example, an annual variation with the amplitude of  $(4.5 \pm 0.8) \cdot 10^{-5}$  was found as a result of a processing of the data collected at 500 days of the Earth's surface measurement with  $^{40}\text{K}$  source in [3]. It was found that this variation corresponds completely to the known annual variation of the cosmic ray intensity and could be explained by cosmic ray background events contribution to the total detector's count rate. A variation with the  $\sim 300$  days period and  $4 \cdot 10^{-5}$  amplitude was found in the data collected during 480 days in the underground measurement with  $^{232}\text{Th}$  source. It was found that this variation correlates with a variation of a daily averaged

dead time per event and could be explained by a modulation of the RC circuit providing the shaping time of the amplifier.

The weak point of the experiments aimed to monitor a stability of a controlled radiation count rate is the high sensitivity to the similar variations of the measurement conditions. It seems that this shortcoming became unimportant for the decay constant determination based on direct registration of a life time of nucleus between birth and decay. This methodics was realized by us in [8] for  $^{214}\text{Po}$  which decays with  $164.3 \mu\text{s}$  half-life [9] by emitting the 7.687 MeV  $\alpha$  particle. This isotope appears mainly in the excited state ( $\sim 87\%$ ) in the  $^{214}\text{Bi}$   $\beta$  decay. Half-lives of the excited levels do not exceed 0.2 ps [10] and they discharge instantly with regard to the scale of  $^{214}\text{Po}$  half-life. Energies of the most intensive  $\gamma$  lines are equal to 609.3 keV (46.1% per decay), 1120 keV (15.0%), and 1765 keV (15.9%). So,  $\beta$  particle and  $\gamma$  quantum are emitted at the moment of a birth of  $^{214}\text{Po}$  nuclear (start) and  $\alpha$  particles are emitted at the decay moment (stop). Measurement of “start-stop” time intervals allows one to construct decay curve at an observation time and to determine the half-life from its shape. The  $^{226}\text{Ra}$  source ( $T_{1/2} = 1600 \text{ yr}$ ) was used as a generator of  $^{214}\text{Bi}$  nuclei which arise in the decay sequence of the mother isotope.

The direct measurement of a nuclear life time allows one moreover to study the radioactive decay law itself. The theoretical models discussed in [11, 12] predict that the decay curves could deviate from the exponential law in the short- and very long-time regions of the time scale. The theoretically predicted [13–15] so-called quantum Zeno effect consisting in a slowing down of the decay rate in a case of constant observations at the decaying object presents a special interest. Experimentally Zeno effect was proved [16] in repeatedly measured two-level system undergoing Rabi transitions but not observed in spontaneous decays.

A limitation of the annual variation amplitude was set at the level of  $3.3 \cdot 10^{-3}$  at the first stage of our measurements [8]. Factors limiting the sensitivity were revealed and ways of its optimization were designed. The improvements of the setups, methods of measurements and data processing, results of an analysis of possible sources of systematic errors were described in [17]. The annual variation with an amplitude of  $(6.9 \pm 3.0) \cdot 10^{-4}$  and the solar-daily variation with an amplitude of  $(10.0 \pm 2.6) \cdot 10^{-4}$  were obtained as a result of a processing of the data collected within 480 days of the measurements.

A brief description of the used installation and results of a broadened analysis of the data collected within 590 days are given in the present work.

## 1. METHOD OF MEASUREMENTS

The TAU-2 setup consists of two scintillation detectors D1 and D2 used in the work. The D1 was made of two glued discs of a plastic scintillator (PS) with the 18 mm diameter ( $d$ ) and 0.8 mm thickness ( $h$ ). A thin transparent circular

bag glued of two 2.5  $\mu\text{m}$  lavesan layers is placed between the discs. A radium spot is deposited preliminary in the center of inner surface of one lavesan circle. The D1 registers  $\beta$  particles from  $^{214}\text{Bi}$  decays and  $\alpha$  particles from  $^{214}\text{Po}$  decays. The massive detector D2 made of NaI(Tl) crystals is intended for the  $\gamma$ -quanta detection. Two NaI(Tl) crystals ( $d = 150$  mm,  $h = 150$  mm) are placed by ends one to another with the 10-mm gap. The D1 is placed into a gap between D2a and D2b. The light collection is fulfilled from a lateral side of the PS disc installed into a deep narrow well with a reflecting wall. The measurements are carried out in the low background room of the underground laboratory DULB-4900 of the BNO INR RAS at the depth of 4900 m of water equivalent [18] in the additional shield made from Pb (15 cm).

Registration of the pulses in the setup is carried out by the two-channel digital oscilloscope La-n20-12PCI which is inserted into a personal computer (PC). Pulses are digitized with 6.25 MHz frequency (160 ns/channel). The DO pulse recording starts by a signal from the D2 which registers  $^{214}\text{Bi}$  decay's  $\gamma$ -quanta. A D2 signal opens a record of a sequence with 655.36  $\mu\text{s}$  total duration where the first 81.92  $\mu\text{s}$  time is a "prehistory" and the last 573.44  $\mu\text{s}$  is a "history". Duration of the "history" exceeds the three  $^{214}\text{Po}$  half-lives.

A scintillation detector D1 in the TAU-2 has a relative  $\alpha/\beta$  light output  $\sim 0.1$  [19]. As a result, the pulses from the  $\alpha$  and  $\beta$  particles have the comparable amplitudes. This circumstance was used to a preliminary selection of the "useful" events by the "on-line" program preparing the data for a PC recording. A number of pulses in the D1 and D2 channels and their delays are obtained. The pulses have been tested for correspondence to the "correct event" criteria such as 1) the only one pulse in the D2 channel, 2) presence of the prompt coinciding pulse in the D1 channel, 3) presence of the only one delayed pulse in the "history" of the D1 channel, and 4) absence of any pulses in the "prehistory" of the D1. The frames not corresponding to the correct event criteria are rejected. A "correct" event appearing time, pulse amplitudes, and its appearing time are recorded into the PC memory. This information allows one to "off line" processing the data for the different regions of pulse amplitudes. A count rate of the "right" events is equal to  $\sim 12$   $\text{s}^{-1}$ . A rate of an information accumulation is equal to  $\sim 25$   $\text{Mb} \cdot \text{day}^{-1}$ .

## 2. SEARCH FOR LONG-DURATION VARIATIONS OF THE TAU-2 DATA

The spectra of the  $\beta$  pulses (spectrum *a*) and  $\alpha$  pulses (spectrum *b*) of the D1 detector and of the  $\gamma$  pulses (spectrum *c*) of the D2 detector, corresponding to the selection conditions mentioned above, are shown in Fig. 1. The peak at the channel  $\sim 1600$  on the spectrum *b* is formed by the 7.69 MeV  $\alpha$  particles. A total time of the data collection is equal to 730 days at the period October 2012 –

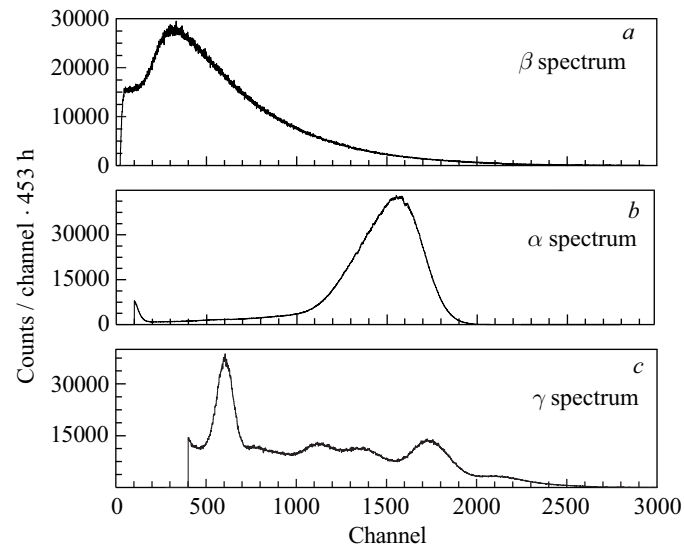


Fig. 1. Spectra of the coincided in  $573.44 \mu\text{s}$  delay of pulses from the detectors D1 ( $a$  —  $\beta$  spectrum) and D2 ( $c$  —  $\gamma$  spectrum) and the  $\alpha$  spectrum (plot  $b$ ) of one of the first pulses D1 to install TAU-2

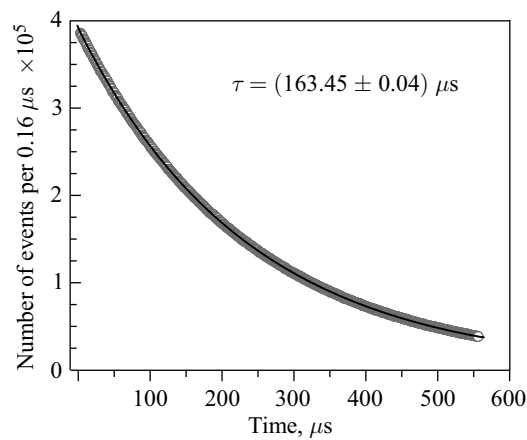


Fig. 2. The start–stop delays distribution obtained in 590 days at the TAU-2. The decay curve of  $^{214}\text{Po}$  with  $\tau = (163.45 \pm 0.04) \mu\text{s}$

October 2014. A decay curve constructed for the total data set is shown in Fig. 2. A value of the  $\tau$  obtained from these data is equal to  $(163.45 \pm 0.04) \mu\text{s}$ . The  $\tau$  value equal to  $(163.58 \pm 0.29 \text{ (stat.)} \pm 0.10 \text{ (syst.)}) \mu\text{s}$  was measured at the Gran Sasso in the recent work [20]. These two values are compatible in the  $1\sigma$  limits.

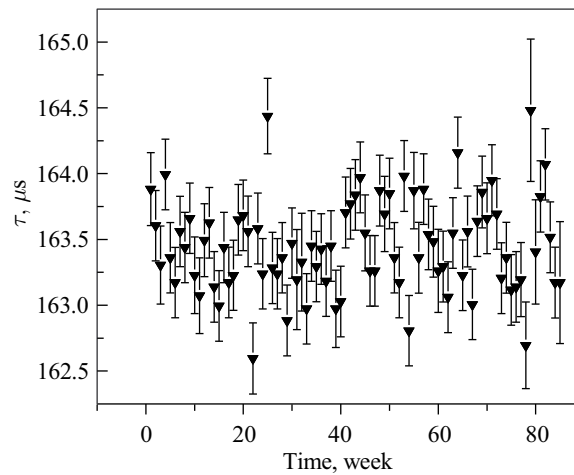


Fig. 3. Dependence on time of the  $\tau$  value obtained at the TAU-2 with the week step

The continuous in time data set was divided into portions of equal length to search for possible time variations. The decay curve has been constructed for each partition data set and the continuous in time sequence of the  $\tau$  values with the specified time step has been found. The time dependence of the  $\tau$  values with the week time step is shown in Fig. 3. The  $\tau$  values were defined for the 3.2–560  $\mu\text{s}$  delay-time region by means of a  $\chi^2$  approximation of the decay curves collected at one week each with an exponential function

$$y = a \exp\left(-\ln(2)\frac{t}{\tau}\right) + b. \quad (1)$$

The moving-average method (moving summation) was used to search for possible time variations of the  $\tau$  values. A time interval with the duration equal to about 0.5 of the expected period is chosen to search for any harmonic component, and the  $\tau$  value is determined for this interval. Then, the interval has shifted for a one step and the procedure is repeated. The 0.5 y interval and the one-week step were chosen to search for the annular variations. A decay curve was constructed for the data collected at 0.5 y and the  $\tau$  value was determined for it. Then, the interval has shifted for one week and a determination was repeated. The result of the analysis is presented in Fig. 4.

Harmonic component is presented in the data as is seen from the figure. The approximation dependence

$$\tau(t) = \tau_0[1 + A \sin(\omega(t + \varphi))], \quad (2)$$

where  $A = 5.4 \cdot 10^{-4}$ ,  $\omega = 2\pi/365 \text{ d}^{-1}$ ,  $\varphi = 83 \text{ d}$ , (since the 1st of January) obtained from the data by means of  $\chi^2$ -method is shown in Fig. 4 too. It is easy

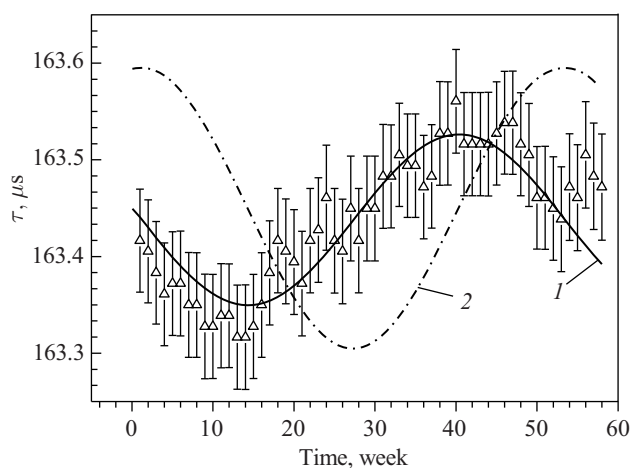


Fig. 4. Distribution in time of  $^{214}\text{Po}$  half-life values obtained by the “moving-average method”. Curve 1 — approximation by function (2) with the parameters:  $A = 5.4 \cdot 10^{-4}$ ,  $\omega = 2\pi/365 \text{ d}^{-1}$ ,  $\varphi = 83 \text{ d}$  (since the 1st of January). Curve 2 — approximation by function (2) with the parameters:  $A = 8.9 \cdot 10^{-4}$ ,  $\omega = 2\pi/365 \text{ d}^{-1}$ ,  $\varphi = 174 \text{ d}$

to show that the original dependence of the week data set has the same period (1 y), the amplitude large at  $\pi/2$  time and shifted at 0.25 y (0.5 of the sliding interval) than the approximation one. The annual wave

$$\tau(t) = \tau_0[1 + 8.9 \cdot 10^{-4} \sin(\omega(t + 174))]$$

obtained in such a way is shown in Fig. 5 together with the week data set of the  $\tau$  values.

It follows from the consideration that the periodic component with the one-year period and the amplitude of

$$A = (8.9 \pm 2.3) \cdot 10^{-4}$$

are presented in the data. The maximum of the periodic function is observed on  $\sim$ October 22. Phases of the obtained period and the period of the Earth–Sun distance variation differ by 3 months. Therefore, obtained periodic variation could not be explained by the distance changing. However, a parameter of the Earth velocity relative to the Sun exists in connection with the Earth–Sun (E.–S.) distance annual variation. A dependence of this parameter is shown in Fig. 5 (curve 2). The obtained annual wave of  $^{214}\text{Po}$  half-life (Fig. 6, curve 1) coincides in phases with the E.–S. velocity dependence within the  $\pm 1$  week accuracy.

The method described above was used to search for the daily variation in the solar, lunar, and sidereal times. A day’s duration was divided into 24 h in each case. The durations of the lunar and sidereal days in the solar time are equal to

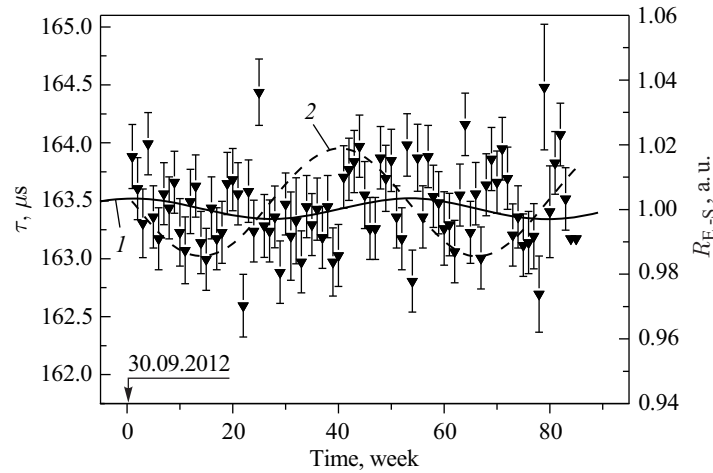


Fig. 5. Distribution in time of  $^{214}\text{Po}$  half-life values for one-week data sets. Curve 1 — approximation by function (2) with the parameters:  $A = 8.9 \cdot 10^{-4}$ ,  $\omega = 2\pi/365 \text{ d}^{-1}$ ,  $\varphi = 174 \text{ d}$ . Curve 2 — time dependence of E-S. distance (right scale)

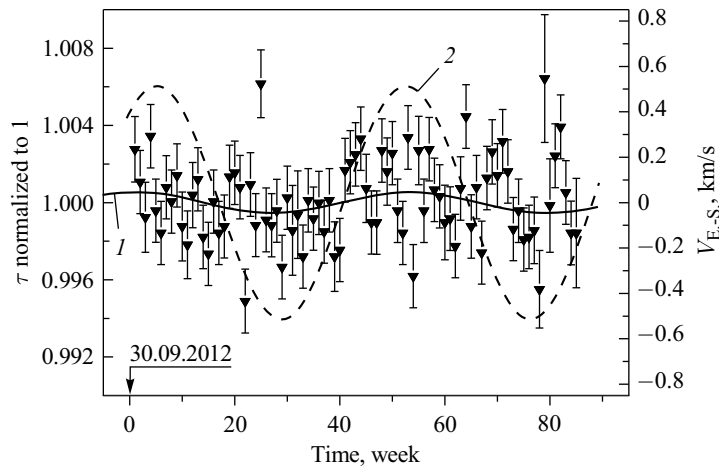


Fig. 6. Normalized to 1 distribution in time of  $^{214}\text{Po}$  half-life values for a week data sets. Curve 1 — approximation by function (2) with the parameters:  $A = 8.9 \cdot 10^{-4}$ ,  $\omega = 2\pi/365 \text{ d}^{-1}$ ,  $\varphi = 174 \text{ d}$ . Curve 2 — time dependence of E. to S. velocity

24 h 50 min 28.2 s and 23 h 56 min 4.09 s, correspondingly [21]. The 12 h duration period was chosen as an averaging interval. All events registered in the 0–12 h interval at the total period of the measurements were used to construct the decay curve. A half-life value was determined from this curve. The interval was

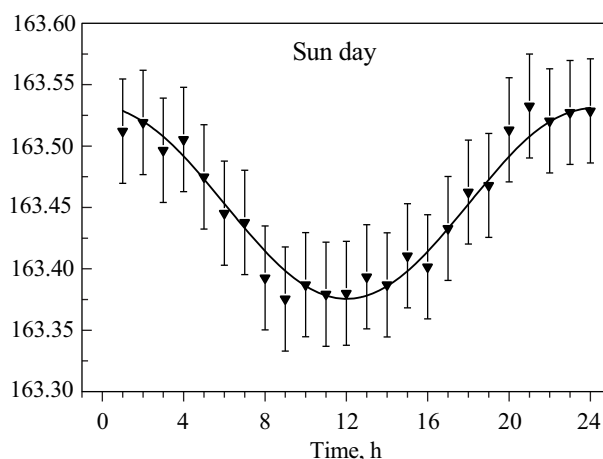


Fig. 7. Solar-daily variation of half-life of  $^{214}\text{Po}$  obtained by means of moving-average method. The solid curve — approximation of function (2) with the parameters:  $A = 4.8 \cdot 10^{-4}$ ,  $\omega = 2\pi/24 \text{ h}^{-1}$ ,  $\varphi = -6 \text{ h}$

moved for 1 h and the procedure was repeated after that. The result of a search for the daily variation in the solar time is shown in Fig. 7 with the parameters ( $A = 4.8 \cdot 10^{-4}$ ,  $\omega = 2\pi/24 \text{ h}^{-1}$ ,  $\varphi = -6 \text{ h}$ ) of the approximation of function (2). The daily variation is described well enough by this sine function as is seen from Fig. 7. A reconstructed sought for dependence

$$\tau(t) = \tau_0 \left[ 1 + 7.5 \cdot 10^{-4} \sin \left( \frac{2\pi}{24} t \right) \right]$$

is shown in Fig. 8 (curve 1) together with a dependence of the Earth surface point velocity relative to the Sun due to the Earth rotation (curve 2). Their phases coincide in the range of  $\pm 0.5 \text{ h}$ . The amplitude of a solar daily variation is equal to  $A_{\text{So}} = (7.5 \pm 1.2) \cdot 10^{-4}$ .

The result of a search for the daily variation  $\tau(t)$  in the lunar time is shown in Fig. 9 (curve 1) with the parameters of the approximation function (2):

$$A = 4.4 \cdot 10^{-4}, \quad \omega = \frac{2\pi}{24} \text{ h}_{\text{ld}}^{-1}, \quad \varphi = 6 \text{ h}_{\text{ld}},$$

where  $\text{h}_{\text{ld}}$  is lunar day hour. The reconstructed sought for dependence

$$\tau(t) = \tau_0 \left[ 1 + 6.9 \cdot 10^{-4} \sin \left( \frac{2\pi}{24} (t + 12) \right) \right]$$

is shown in Fig. 9 (curve 2) together with a dependence of the Earth surface point velocity relative to the Moon due to the Earth rotation (curve 3). Phases of the curves (2) and (3) coincide in the range of  $\pm 0.5 \text{ h}$ . The amplitude of lunar daily variation is equal to

$$A_{\text{L}} = (6.9 \pm 2.0) \cdot 10^{-4}.$$

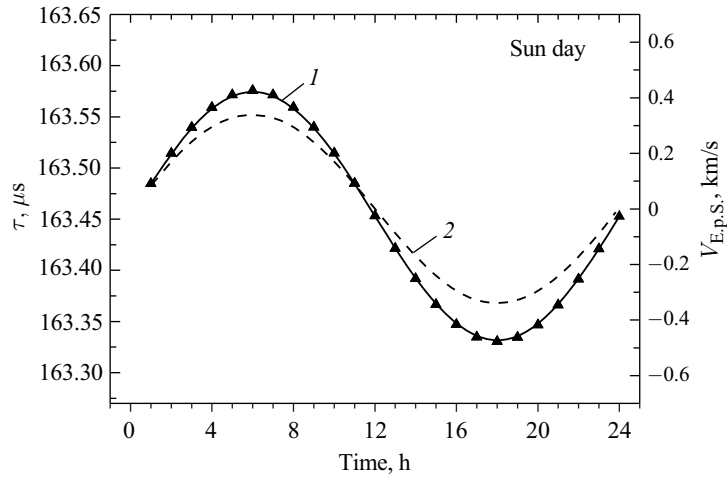


Fig. 8. Curve 1 — solar-daily variation of half-life of  $^{214}\text{Po}$  approximated by function (2) with the parameters:  $A = 7.5 \cdot 10^{-4}$ ,  $\omega = 2\pi/24 \text{ h}^{-1}$ ,  $\varphi = 0 \text{ d}$ . Curve 2 — Earth surface point velocity relative to the Sun due to the Earth rotation

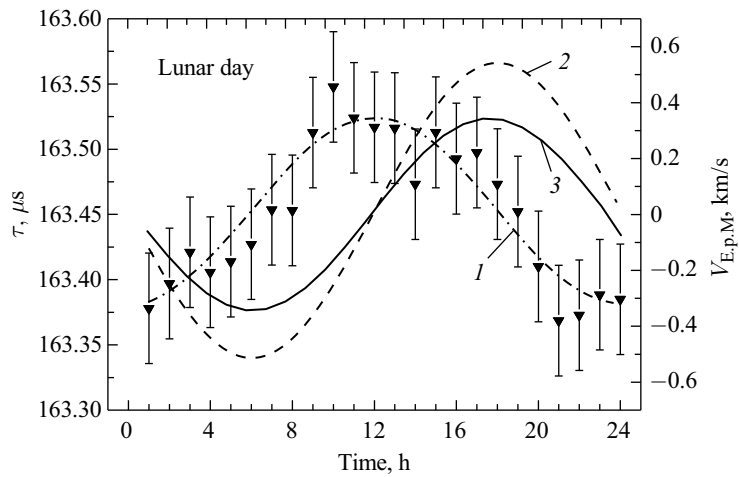


Fig. 9. Lunar-daily variation of half-life of  $^{214}\text{Po}$  obtained by means of moving-average method. The data set starting point is 24:00, 30 September 2012. 1 — approximation function Eq. (2) with the parameters:  $A = 4.4 \cdot 10^{-4}$ ,  $\omega = 2\pi/24 \text{ h}_{\text{ld}}^{-1}$ ,  $\varphi = 6 \text{ h}_{\text{ld}}$ . 2 — sought lunar-daily variation  $\tau(t) = \tau_0[1 + 6.9 \cdot 10^{-4} \sin((2\pi/24)(t + 12))]$ . 3 — Earth surface point velocity ( $V_{E,p,M}$ ) relative to the Moon due to the Earth rotation

Test of a real presence of the lunar daily variation in the data set was done. A starting point of the data summation was shifted at 15 days. A phase of the variation should shift at  $\sim 12 \text{ h}$  because of a difference in time duration of solar

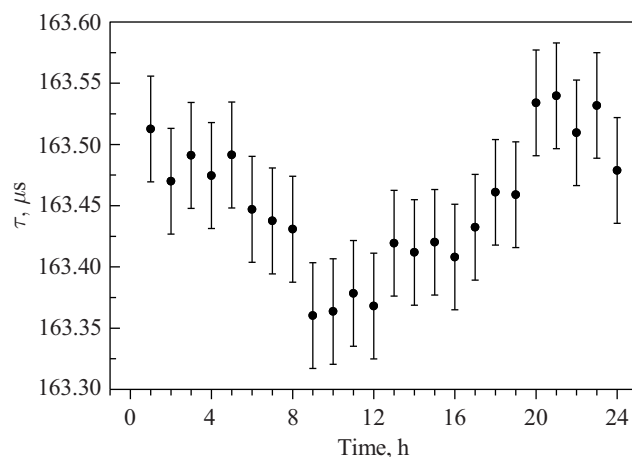


Fig. 10. Lunar-daily variation of half-life of  $^{214}\text{Po}$  obtained by means of moving-average method. Starting point shifted for 15 days (15 October 2012)

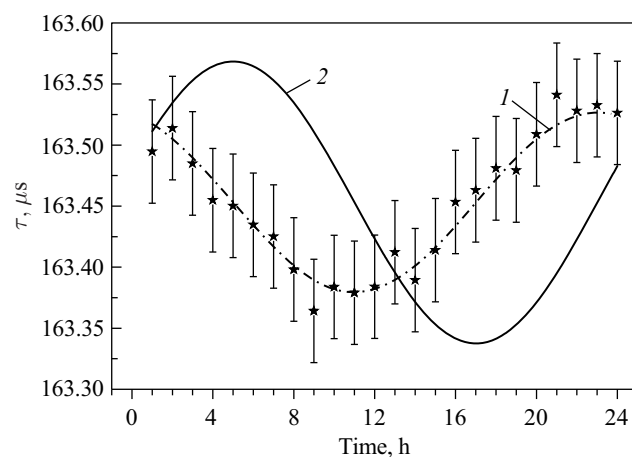


Fig. 11. Sidereal-daily variation of half-life of  $^{214}\text{Po}$  obtained by means of moving-average method. Curve 1 — function Eq. (2) with the parameters:  $A = 4.6 \cdot 10^{-4}$ ,  $\omega = 2\pi/24 \text{ h}_{\text{sd}}^{-1}$ ,  $\varphi = -6 \text{ h}_{\text{sd}}$ . Curve 2 — sought SD variation  $\tau(t) = \tau_0[1 + 7.2 \cdot 10^{-4} \sin((2\pi/24)t)]$

and lunar days ( $(50 \text{ min } 28.2 \text{ s}) \cdot 15 \approx 12 \text{ h}$ ). The result is shown in Fig. 10. A phase had shifted at 12 hours as was waited for a real lunar daily variation.

The result of a search for the daily variation  $\tau(t)$  in the sidereal time is shown in Fig. 11 (curve 1) with the parameters of the approximation function (2):

$$A = 4.6 \cdot 10^{-4}, \quad \omega = \frac{2\pi}{24} \text{ h}_{\text{ld}}^{-1}, \quad \varphi = -6 \text{ h}_{\text{ld}},$$

where  $h_{sd}$  is sidereal day hour. The reconstructed sought for dependence

$$\tau(t) = \tau_0 \left[ 1 + 7.2 \cdot 10^{-4} \sin \left( \frac{2\pi}{24} t \right) \right] \quad (3)$$

is shown in Fig. 11 (curve 2) too. The amplitude of a sidereal daily variation is equal to

$$A_S = (7.2 \pm 1.2) \cdot 10^{-4}.$$

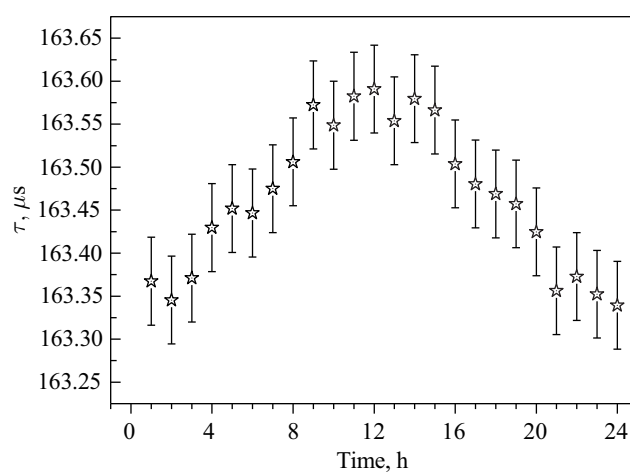


Fig. 12. Sidereal-daily variation of half-life of  $^{214}\text{Po}$  obtained by means of moving-average method. Starting point shifted for 182 days

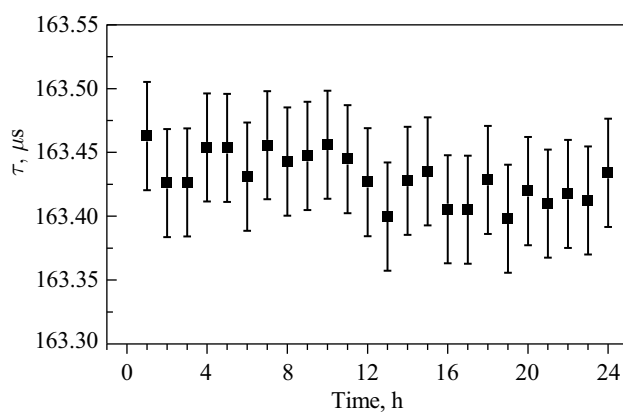


Fig. 13. Anti-sidereal-daily variation of half-life of  $^{214}\text{Po}$  obtained by means of moving-average method.  $d_{asd} = d + \Delta t = 24 \text{ h } 3 \text{ min } 55.9 \text{ s}$

It was done as test of a real presence of the sidereal daily variation in the data set. A starting point of the data summation was shifted at 182 days. A phase of the variation should shift at  $\sim 12$  h because of the difference in time duration of solar and sidereal days ( $(3 \text{ min } 55.9 \text{ s}) \cdot 182 \approx 12 \text{ h}$ ). The result is shown in Fig. 12. A phase had shifted at 12 h as was waited for a real sidereal daily variation.

The possibility of a stochastic realization of sidereal variation was tested as well. The analysis was repeated for an artificial anti-sidereal day. Its duration in the solar time is equal to 24 h 3 min 55.9 s. The result of the analysis is shown in Fig. 13. No variation is seen within the statistical errors. It gives a confidence that the sidereal daily variation is really present in the data. It is difficult to correlate the sidereal daily variation with any cosmic object at present time because the nature of the possible influence is unknown. Nevertheless, if such an object exists then it should be an annual variation connected with it. The question needs additional investigation.

### 3. RESULTS AND DISCUSSION

The moving-average method was used to search for annual and daily variations because of a need to improve the statistics of analyzed decay curves and to increase multiplying the sensitivity of the analysis to a value of a possible variation. As is seen from the comparison of the data in Figs. 3 and 4, a value of a statistical error was decreased  $\sim 5$  times by increasing the data accumulation interval from one week up to 26 weeks (0.5 yr). Using of the Fourier-method and wavelet method in the analysis is complicated by a relatively short size of the time series. Besides, a time  $\tau$ -series could include not only annual variation but, for example, semiannual one. The integrated dependence lost the unambiguity in this case. The used method targeted at a search for the specific variation determined a univocal binding exactly. It is necessary to compare obtained set of the  $\tau$  values with similar data measured independently on the other similar setup to find a confidence that the variations are nonrandom. Such measurements are carried out in the BNO INR RAS with the TAU-1 setup since May 2014. The setup is placed in the low-background laboratory CAPRIZ at 1000 m w.e. depth. The statistics needed to carry out the comparison of coincidence behavior of the  $\tau$  values time sets is accumulated. It is clear that an essential improvement of the statistics could be achieved by a multiple increasing of the dataset rate. The quadratic increase of a random coincidence fraction will occur for the used  $^{214}\text{Po}$  source in the case of a considerable growth of its activity. The value of random coincidence is equal to 1% at  $12 \text{ s}^{-1}$  dataset rate. Such a large value is connected with a high total activity of all  $^{226}\text{Ra}$  daughter elements in the source and relatively long half-life of  $^{214}\text{Po}$ . Because of it, an increase of dataset rate for  $^{214}\text{Po}$  without relative growth of a random coincidence background is possible by means of increasing the number of independent measuring setups. This variant

seems hardly feasible. Another possibility could be realized by using a pair of radioactive isotopes with a similar decay scheme but a shorter half-life. The pair  $^{213}\text{Bi}$ – $^{213}\text{Po}$  ( $T_{1/2} = 4.2 \mu\text{s}$ ) is a good candidate for such a source. These isotopes are the daughter products of  $^{229}\text{Th}$  ( $T_{1/2} = 7340 \text{ yr}$ ) [10] which would be used as a generator isotope. The preparation of the new setup for  $^{229}\text{Th}$  is carried out at the BNO INR RAS at present time.

## CONCLUSIONS

The results of the data analysis obtained with the TAU-2 setup at the new step of measurements are shown in this paper. The setup is intended for carrying out a long-duration control at a value  $^{214}\text{Po}$  half-life constant. The methods of measurement and processing of collected data are reported. Results of the analysis of time series values of  $\tau$  with different time step are presented. Total time of measurements was equal to 730 days. Averaged at 590 days value,  $^{214}\text{Po}$  half-life was found  $T_{1/2} = (163.46 \pm 0.04) \mu\text{s}$ . It is shown that the constant feels the daily and annual variations of the unknown nature. The annual variation with an amplitude  $A = (8.9 \pm 2.3) \cdot 10^{-4}$ , solar-daily variation with an amplitude  $A_{\text{So}} = (7.5 \pm 1.2) \cdot 10^{-4}$ , lunar-daily variation with an amplitude  $A_L = (6.9 \pm 2.0) \cdot 10^{-4}$ , and sidereal-daily variation with an amplitude  $A_S = (7.2 \pm 1.2) \cdot 10^{-4}$  were found in a series of  $\tau$  values. The maximal values of amplitude are observed at the moments when the projections of the installation Earth location velocity vectors toward the source of possible variation achieve their maximal magnitudes. The measurements are continuing.

The work was made in accordance with INR RAS and V.N. Karazin KhNU plans of the Research and Developments.

## REFERENCES

1. Hardy J. C., Goodwin J. R., Iacob V. E. Do Radioactive Half-Lives Vary with the Earth-to-Sun Distance? // *Appl. Rad. Isot.* 2012. V. 70. P.1 931; arXiv:1108.5326 [nucl-ex]; doi: 10.1016/j.apradiso.2012.02.021.
2. Bellotti E. et al. Search for the Time Dependence of the  $^{137}\text{Cs}$  Decay Constant // *Phys. Lett. B.* 2012. V. 710. P. 114; arXiv:1202.3662 [nucl-ex]; doi: 10.1016/j.physletb.2012.02.083.
3. Bellotti E. et al. Search for Time Modulations in the Decay Rate of  $^{40}\text{K}$  and  $^{232}\text{Th}$  and Influence of a Scalar Field from the Sun // *Astropart. Phys.* 2014. V. 61. P. 82; arXiv:1311.7043 [astro-ph.SR]; doi: 10.1016/j.astropartphys.2014.05.006.
4. Jenkins J. H. et al. Evidence for Correlations between Nuclear Decay Rates and Earth–Sun Distance // *Astropart. Phys.* 2009. V. 32. P. 42; arXiv:0808.3283 [astro-ph]; doi: 10.1016/j.astropartphys.2009.05.004.

5. *Sturrock P. A., Fischbach E., Jenkins J.* Analysis of Beta-Decay Rates for Ag-108, Ba-133, Eu-152, Eu-154, Kr-85, Ra-226 and Sr-90, Measured at the Physikalisch-Technische Bundesanstalt from 1990 to 1996 // *Astrophys. J.* 2014. V. 794. P. 42; arXiv:1408.3090 [nucl-th]; doi: 10.1088/0004-637X/794/1/42.
6. *Sturrock P. A. et al.* Comparative Study of Beta-Decay Data for Eight Nuclides Measured at the Physikalisch-Technische Bundesanstalt // *Astropart. Phys.* 2014. V. 50. P. 47; doi: 10.1016/j.astropartphys.2014.04.006.
7. *Nahle O., Kossert K.* Comment on Comparative Study of Beta-Decay Data for Eight Nuclides Measured at the Physikalisch-Technische Bundesanstalt [*Astropart. Phys.*, 50, 47–58] // *Astropart. Phys.* 2015. V. 66. P. 47; arXiv:1408.5219 [nucl-ex]; doi: 10.1016/j.astropartphys.2014.11.005
8. *Alexeyev E. N. et al.* Experimental Test of the Time Stability of the Half-Life of Alpha-Decay Po-214 Nuclei // *Astropart. Phys.* 2013. V. 46. P. 23; arXiv:1112.4362 [nucl-ex]; doi: 10.1016/j.astropartphys.2013.04.005.
9. *Wu S.-C.* Nuclear Data Sheets for  $A = 214$  // *Nucl. Data Sheets.* 2009. V. 110. P. 681; doi: 10.1016/j.nds.2009.02.002.
10. *Firestone R. B., Frank Chu S. Y.* Table of Isotopes / Ed. by Baglin C. M., 8th ed. New York: Willey, 1996.
11. *Gopych P. M., Zaljubovsky I. I.* // *Phys. Part. Nucl.* 1988. V. 19. P. 785.
12. *Fonda L., Ghirardi G. C., Rimini A.* Decay Theory of Unstable Quantum Systems // *Rep. Prog. Phys.* 1978. V. 41. P. 587; doi: 10.1088/0034-4885/41/4/003.
13. *Khalfin L. A.* Zeno's Quantum Effect // *Sov. Phys. Usp.* 1990. V. 33, No. 10. P. 868–869 (*Usp. Fiz. Nauk.* 1990. V. 160, No. 10. P. 185).
14. *Misra B., Sudarshan E. C. G.* The Zeno's Paradox in Quantum Theory // *J. Math. Phys.* 1977. V. 18. P. 756.
15. *Facchi P., Pascazio S.* Quantum Zeno Dynamics: Mathematical and Physical Aspects // *J. Phys. A: Math. Theor.* 2008. V. 41. P. 493001; doi: 10.1088/1751-8113/41/49/493001.
16. *Itano W. M. et al.* Quantum Zeno Effect // *Phys. Rev. A.* 1990. V. 41. P. 2295; doi: 10.1103/PhysRevA.41.2295.
17. *Alexeyev E. N. et al.* Sources of the Systematic Errors of  $^{214}\text{Po}$  Half-Life Measurements // *Phys. Part. Nucl.* 2015. V. 46, No. 2. P. 157; arXiv:1404.5769 [nucl-ex]; doi: 10.1134/S1063779615020021.
18. *Gavriljuk Ju. M. et al.* Working Characteristics of the New Low-Background Laboratory (DULB-4900, Baksan Neutrino Observatory) // *Nucl. Instr. Meth. A.* 2013. V. 729. P. 576; arXiv:1204.6424 [physics.ins-det]; doi: 10.1016/j.nima.2013.07.090.
19. *Medvedev M. N.* // Report from Gravity Works in the Baksan Valley in 2013. Report SAI, Moscow, 2013.
20. *Bellini G. et al. (BOREXINO Collab.).* Lifetime Measurements of  $^{214}\text{Po}$  and  $^{212}\text{Po}$  with the CTF Liquid Scintillator Detector at LNGS // *Eur. Phys. J. A.* 2013. V. 491. P. 92; arXiv:1212.1332 [nucl-ex]; doi: 10.1140/epja/i2013-13092-9.
21. Explanatory Supplement to the Astronomical Almanac (at page 698) / Ed.: P. Kenneth Seidelmann. United States Naval Observatory. Nautical Almanac Office, Great Britain, 1992.